*International Journal of Advancements in Electronics and Electrical Engineering– IJAEEE*
*Volume 4 : Issue 1* [ISSN : 2319-7498]
*Publication Date : 30 April, 2015*

# Turbo Coding over Nakagami-m Fading Channels

Kovaci Maria, Balta Horia

***Abstract*—Nakagami-*m* channels are communication channels that can be modeled using the Nakagami-*m* distribution. The Nakagami-*m* distribution provides a wide range of models for channels exhibiting fading (fluctuating channels). By suitably choosing the *m* parameter, a certain fading intensity/strength can be simulated. This paper aims to assess the performance of different types of turbo-codes (TC) over Nakagami channels.**

***Keywords*—comunication sistems, turbo codes; Nakagami-*m* distribution; flat fading channels; bit error rate**

## I. Introduction

Most current wireless communication systems face the problem of fading. A typical radio channel exhibits multipath reception, which causes fading [1]. If the channel transfer function is sufficiently constant over the signal bandwidth then we are dealing with flat fading (or frequency nonselective fading). This corresponds to the assumption that intersymbol interference does not play a major role in the performance of the radio links. The presence of fading diminishes the quality of transmissions. Methods to combat frequency selective fading are based on (turbo-)equalization [2]. Protection coding (forward error correction – FEC coding) is an effective method to combat the flat fading effect. Coding gains tens of dB. This paper takes into consideration flat fading.

Coding optimization for fading channels involves simulations and, implicitly, fading modeling. Purely fluctuating channel modeling is based on Rayleigh's distribution. A purely fluctuating channel is a channel in which the received signal is composed only of the reflected waves that can be modeled by random independent and identically distributed (i.i.d.) variables. A channel without fading (non-fluctuating) provides a direct path (line of sight) between the transmitter and receiver. In most actual cases, the received signal contains comparable proportions of both the fluctuating and non-fluctuating component. Modeling this situation calls for Rice's distribution.

Rician fading assumes a dominant line-of-sight component and a large set of i.i.d. reflected waves. Reflected waves arrive with a random phase offset and the accumulation can be modeled as a phasor addition of signals with random amplitude and phase [3]. The received signal amplitude has the probability density function (pdf):

$$f_{Rice}(x) = \frac{2(K+1)x}{\Omega} \cdot \exp\left(-K - \frac{(K+1)x^2}{\Omega}\right) \cdot I_0\left(2\sqrt{\frac{K(K+1)}{\Omega}}x\right). \quad (1)$$

where $K$ is the ratio between the power in the direct path and the power in the other, scattered, paths; $\Omega$ is the total power from both paths and acts as a scaling factor to the distribution; and $I_0(.)$ is the 0th order modified Bessel function of the first kind.

An alternative to Rician channel modeling with varying degrees of (intensity of) fading is using Nakagami's distribution [4]. The Nakagami-*m* distribution can be used to model fading channel conditions that are either more or less serve than the Rayleigh distribution, and it includes the Rayleigh distribution as a special case ($m$=1). For analytical and numerical evaluation of system performance, the expressions for Rician fading are less convenient, mainly due to the occurrence of a Bessel function in the Rician probability density function of received signal amplitude. Approximations by a Nakagami distribution, with simpler mathematical expressions have become popular.

In the present study, we investigated by means of simulations the performance of turbo coding over the Nakagami channel with different degrees of fading (identified by parameter $m$ – the fading figure).

We used single-binary, duo-binary and multi-non-binary turbo codes.

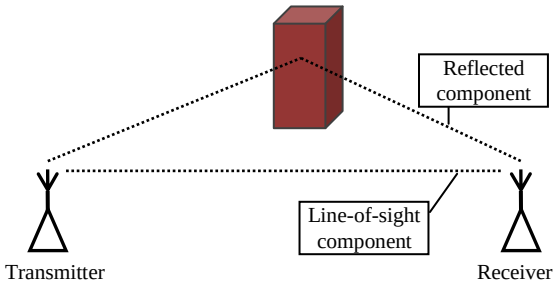


Figure 1. Example of multipath propagation in transmission radio channel.

M. Kovaci
Electronics and Telecommunication Faculty, University Politehnica Timisoara
Timisoara, Romania

H. Balta
Electronics and Telecommunication Faculty, University Politehnica Timisoara
Timisoara, Romania



SEEK DIGITAL LIBRARY

The rest of the paper is structured as follows. In section II, we present the Nakagami-*m* distribution and its mode of generation. Section III describes TCs used in simulations, whose results are presented in Section IV. Section V concludes the paper.

## II. The Nakagami Channels

In contrast to common belief, the Nakagami model is not an appropriate approximation for Rician fading. It has an essentially different behaviour for deep fades, such that results on outage probabilities or error rates can differ by orders of magnitude [3]. The Nakagami fading model was initially proposed because it matched empirical results for short wave ionospheric propagation. In current wireless communication, the Nakagami model describes the amplitude of received signal after maximum ratio diversity combining.

The sum of multiple i.i.d. Rayleigh-fading signals have a Nakagami distributed signal amplitude. This is particularly relevant to model interference from multiple sources. The Rician and the Nakagami model behave approximately equivalently near their mean value.

The Nakagami- *m* pdf is given by:

$$p_N(\alpha) = \frac{2 \cdot m^m}{\Gamma(m)} \cdot \frac{\alpha^{2m-1}}{\left(2\sigma^2\right)^m} \cdot \exp\left(-m\frac{\alpha^2}{2\sigma^2}\right) \qquad (2)$$

where $m \geq 1/2$ represents the fading figure.

The mean, $\overline{\alpha}$, and the value of the mean square, $\overline{\alpha^2}$, for $m \geq 1$, integer, are the following:

$$\overline{\alpha} = \sqrt{2\sigma^2} \cdot \sqrt{\frac{\pi}{4m}} \cdot P, \quad \overline{\alpha^2} = 2\sigma^2 \qquad (3)$$

where $P$=1 for $m$=1 and $P = \prod_{i=1}^{m-1} \frac{2i+1}{2i}$ for $m$≥2.

To modelate the fading channel, a sufficient and acceptable model is to consider the input-output relation of the digital channel of the form:

$$y_k = \alpha_k \cdot x_k + z_k, \qquad (4)$$

where $x_k$ and $y_k$ are the transmitted and received data for the time slot $k$, respectively; the parameter $\alpha_k$ is a random value which is characterized the time fluctuations from symbol to symbol (fast fading) or from block to block (block fading). Its distribution determines the channel type: Rayleigh, Rice or Nakagami. The input sequence $\{x_k\}$ is binary, random, in NRZ bipolar format, i.e. with unitary variance. Finally, the samples $z_k$ are zero-mean i.i.d. Gaussian variables of variance $\sigma^2$.

To generate the random variable $\alpha$, in simulations, we used the method described in [5]. For comparison with the simulations presented in Section IV, Fig. 2 shows the bit error rate (BER) performance of Nakagami channels for $m$ = 2, 3, 4, and 5, and of the AWGN channel without the use of FEC encoding.

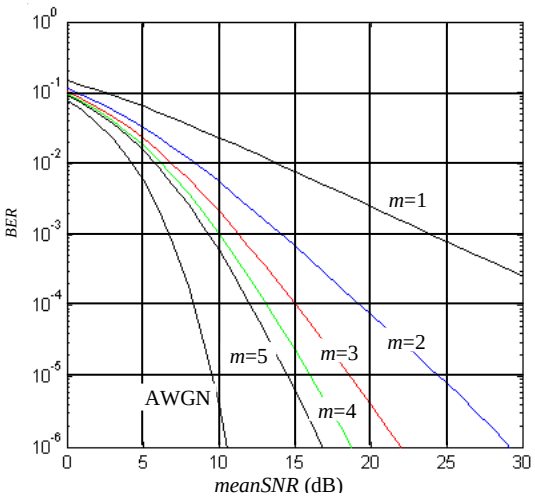


Figure 2. The BER performances obtained through the simulation of the BPSK modulation transmission system on the Nakagami flat fading channels, with $m$ = 2, 3, 4 and 5.

## III. Multi-Non-Binary Turbo Codes

Having defined the channel model, we further briefly present TCs involved in simulations performed. We considered single binary (SBTC), double binary (DBTC) and multi-non-binary (MNBTC) turbo codes.

Because they differ by their component convolutional encoder (CE), we further present a general scheme and customizations required for each case. Fig. 3 shows the general scheme of a memory-$M$ recursive systematic multi-non-binary convolutional encoder, with a rate $R_c$=$R$/($R$+1). This scheme is known as the observer canonical form [6]. The encoder has $R$ non-binary inputs taking values in the Galois field GF($2^Q$), and is then referred to as a multi-non-binary (MNB). Each cell of the register in Fig. 3 stores a vector of $Q$ bits at a time. All the links are supposed to have a width equal to $Q$ in order to carry $Q$-bit vectors, [7]. The generator polynomial coefficient is denoted as $g_{w,r}$ with $0 \leq w \leq M$, $0 \leq r \leq R$. At time $n$, the encoder has $R$ inputs, which consist of a word of symbols $u^n = \left[u_R^n \quad u_{R-1}^n \quad \ldots \quad u_1^n\right]$ with $u_r^n = \left[u_{r,Q-1}^n \quad \ldots \quad u_{r,1}^n \quad u_{r,0}^n\right]$, $1 \leq r \leq R$, $0 \leq n < N$, where $N$ is the inter-symbol interleaving length and $u_{r,q}^n$ are binary coefficients, and $R$+1 outputs corresponding to the $R$ inputs and one redundant symbol $u_0$.

Let $S^n = \left[S_{M-1}^n \quad \ldots \quad S_1^n \quad S_0^n\right]$ denote the encoder state vector at time lag $n$. The input-output relationship of the encoder at time $n$ can be expressed in the compact form, [8]:



SEEK DIGITAL LIBRARY

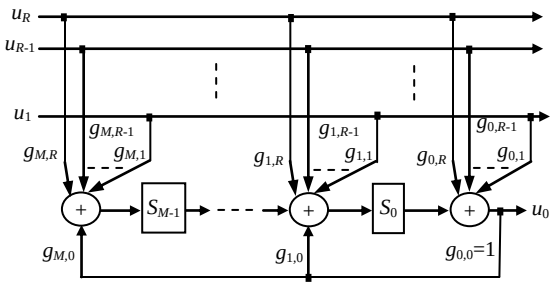


Figure 3. Observer canonical form - General scheme of a memory-$M$ recursive systematic multi-non-binary convolutional encoder, with a rate $R_c=R/(R+1)$.

$$\begin{aligned}\left(S^{n+1}\right)_{1\times M} &= \left(u^n\right)_{1\times R}\cdot\left(G_T\right)_{R\times M} + \left(S^n\right)_{1\times M}\cdot\left(T\right)_{M\times M}\\ u_0^n &= u^n\cdot G_L + S^n\cdot W\end{aligned}, \quad (5)$$

where $G_T = G_L\cdot G_F + G_0^T$, with $G_0^T$ denoting the transpose of $G_0$, $T=\begin{bmatrix}0_{(M-1)\times 1} & I_{M-1}\\ & G_F\end{bmatrix}$ and $W=\left(\begin{bmatrix}0 & 0 & \dots & 0 & 1\end{bmatrix}_{1\times M}\right)^T$, $G_F=\begin{bmatrix}g_{M,0} & g_{M-1,0} & \dots & g_{1,0}\end{bmatrix}$, $G_L=\begin{bmatrix}g_{0,R} & g_{0,R-1} & \dots & g_{0,1}\end{bmatrix}^T$, and $G_0=\begin{bmatrix}g_{w,r}\end{bmatrix}_{M\ge w\ge 1,\ R\ge r\ge 1}$.

The descriptive matrix of the implementation form (*dif-matrix*), $G$, is defined as follows:

$$G=\begin{bmatrix}G_0 & G_F^T\\ G_L^T & 1\end{bmatrix}=\begin{bmatrix}g_{w,r}\end{bmatrix}_{M\ge w\ge 0,\ R\ge r\ge 0}. \quad (6)$$

# IV. Simulation Results

We begin by specifying parameters for TCs used in simulations. They are succinctly shown in Table I. As mentioned above, the CE component is described by dif-matrix G. Because the theory developed for MNBTCs can be particularized for others TC families we simple indicate the dif-matrix in each case. Thus for a single binary convolutional encoder (SBCE) the dif-matrix has the size $M\times 2$ and for doubly-binary convolutional encoder (DBCE) the dif-matrix has the size $M\times 3$. Both of them have binary entries. For multi-non-binary convolutional encoder (MNBCE), the dif-matrix entries are from GF(4).

For a fair comparison, we chose the same number of information bits per block (1504) in all three cases. For the SBTC, a data block consists of a binary vector whose length is equal to that of the interleaver. As such, for the SBTC, we have only inter-symbol interleaving performed by a quadratic polynomial permutation (QPP) type interleaver. The QPP interleaver can be expressed as, [8]:

$$\pi(i)=\left(f_1\cdot i+f_2\cdot i^2\right)\bmod N,\quad 0\le i<N, \quad (7)$$

TABLE I. TC'S PARAMETERS USED IN SIMULATIONS

| parameter | SBTC | DBTC | MNBTC |
|---|---|---|---|
| Component CE ($G$ matrix) | $\begin{bmatrix}1&1\\1&0\\0&0\\0&1\\1&1\end{bmatrix}$ | $\begin{bmatrix}1&1&1\\0&0&1\\1&1&0\\0&1&0\\1&1&1\end{bmatrix}$ | $\begin{bmatrix}3&2&2\\1&1&1\\2&2&1\\1&1&1\end{bmatrix}$ |
| Data block size $R\times Q\times N$ (bits) | 1×1×1504 | 2×1×752 | 2×2×376 |
| Inter-symbol interleaver | QPP with $f_1$=49, $f_2$=846 | ARP defined in [10] | QPP with $f_1$=45, $f_2$=94 |
| Intra-symbol interleaving | – | defined in [10] | Helical, defined in [7] |
| Trellis closure | UDT | Tail biting | |
| Modulation | BPSK | | |
| Decoding algorithm | Max-Log-MAP | | |
| Scaling coefficient | 0.7 | 0.75 | 0.75 |
| Stopping criterion | genie | | |
| Maximum number of iteration | 100 | | |

where $f_1$ and $f_2$ are taken from [9] (pag. 14, Table 5.1.3-3) for both SBTC (with interleaving length of 1504) and MNBTC (with interleaving length of 376). For the DBTC and MNBTC, we also performed an intra-symbol interleaving. For the DBTC, both inter-symbol and intra-symbol interleaving are indicated in the DVB-RCS2 standard [10]. In all cases we used a binary phase shift keying (BPSK) modulation. We used a circular (tail-biting) closure of trellis [11] for MNBTC and DBTC and uninterleaved dual termination (UDT) for SBTC (as in LTE standard, [9]). In all cases we employed the Max-Log-MAP decoding algorithm [12]. For the extrinsic information scaling coefficient we choose values equal to 0.75 for DBTC and MNBTC and an extrinsic information scaling coefficient equal to 0.7 for SBTC [13].

To obtain the curves, we performed simulations until 500 erroneous blocks were obtained or until a maximum number of blocks equal to $10^9$ were simulated. The maximum number of iterations is set to 100, and the genie stopping criterion was used for all cases [14].

Diagrams in Fig. 4 show bit error rate and frame error rate performances versus signal to noise ratio of the above TCs over Nakagami (fluctuating) channels with $m$ = 1, 2, 3, 4, and 5, and for the AWGN channel.

# V. Conclusions

Some conclusions are drawn from the results presented in the previous section. Firstly, we notice the huge gains turbo coding offers. Thus, if the curves in Fig. 2 cross the horizontal corresponding to $BER = 10^{-6}$ at SNR average values between 17 dB for $m$ = 5 and 29 dB for $m$ = 2, turbo coding translates these points to mean SNR values of between 2.1 dB and 3.2 dB. For all cases investigated, regardless of the value of $m$, the same hierarchy of performances in the water fall region is kept, as well as the same behavior in the error floor region. In the water fall region, the DBTC displays the best performance, followed by the SBTC. The differences, however, are



SEEK DIGITAL LIBRARY

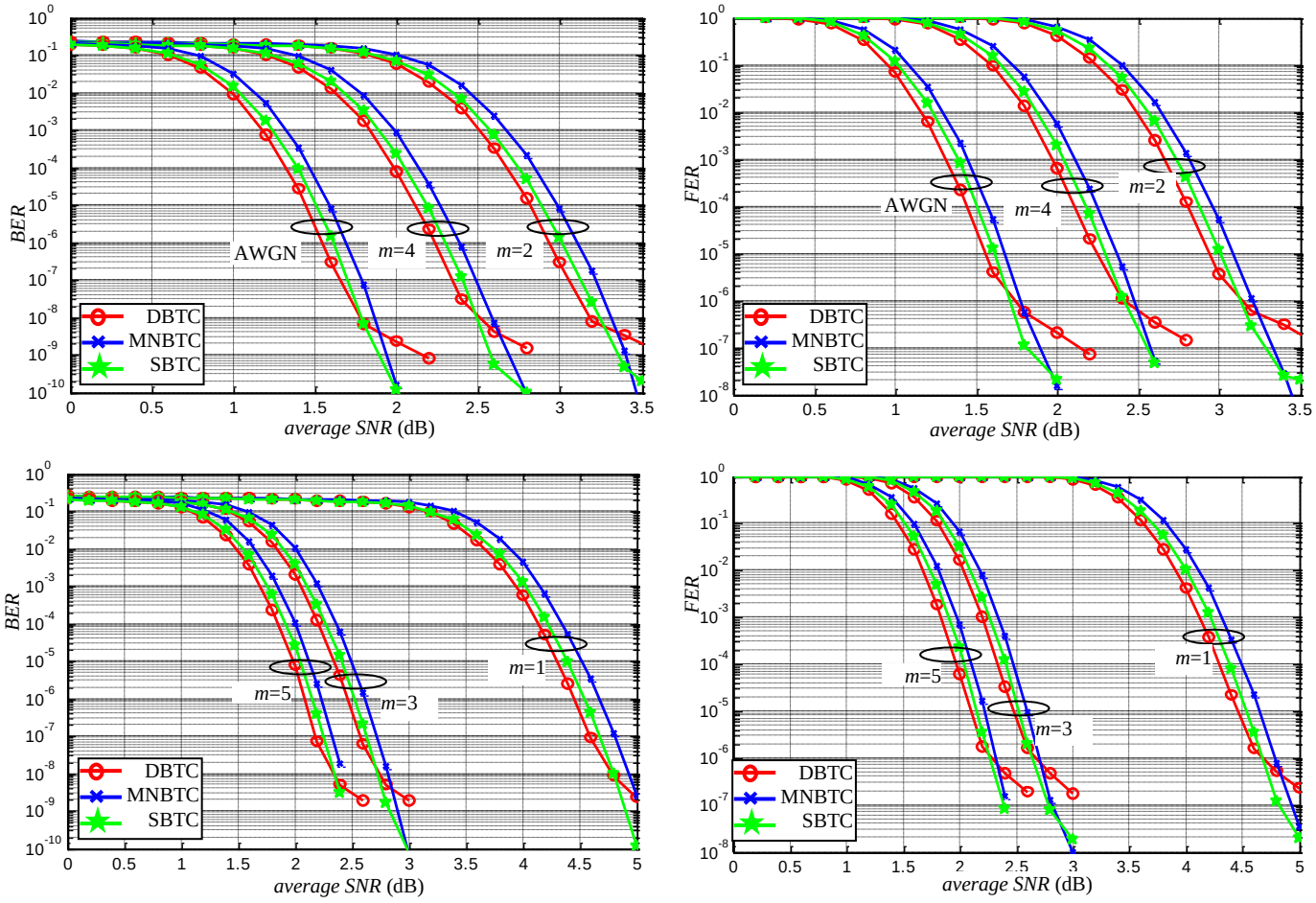


Figure 4. BER/FER versus SNR performance comparison for SBTC, DBTC and MNBTC in flat fading Nakagami channel.

considerably lower than 0.1 dB. Instead, the DBTC has a modest behavior in the error floor region as compared to SBTC and MNBTC. For the MNBTC there is virtually no error floor effect in the BER and FER values investigated.

## Acknowledgment

This work was partially supported by the strategic grant POSDRU/159/1.5/S/137070 (2014) of the Ministry of National Education, Romania, co-financed by the European Social Fund – Investing in People, within the Sectoral Operational Programme Human Resources Development 2007-2013 and by a grant of the Romanian Ministry of Education, CNCS – UEFISCDI, project number PN-II-RU-PD-2012-3-0122.

## References

[1] J.G. Proakis, Digital Communications, McGrawHill; 4th edition (2000)

[2] C. Douillard, M. Jezequel, and C. Berrou, Iterative Correction of Intersymbol-Interference: Turbo-Equalization, European Transactions on Telecommunications, Volume 6, Issue 5, pages 507-511, September/October 1995.

[3] http://www.wirelesscommunication.nl/reference/chaptr03/ricenaka/ricenaka.htm

[4] Nakagami, M. (1960) "The m-Distribution, a general formula of intensity of rapid fading". In William C. Hoffman, editor, Statistical Methods in Radio Wave Propagation: Proceedings of a Symposium held June 18-20, 1958, pp 3-36. Pergamon Press.

[5] Asilomar H. Balta, M. Kovaci, A. De Baynast "Performance of Turbo-Codes on Nakagami Flat Fading (Radio) Transmission Channels", Signals, Systems and Computers, 2005. Conference Record of the Thirty-Ninth Asilomar Conference on October 28 - November 1, 2005, pp. 606 – 610.

[6] T Kailath, Linear Systems, Prentice-Hall, Upper Saddle River, 1980.

[7] H. Balta, C. Douillard and R. Lucaciu, "Multi-non-binary turbo codes" EURASIP Journal on Wireless Communications and Networking, volume 2013.

[8] H. Balta, C. Douillard, and A. Isar, "On the Equivalence Between Canonical Forms of Recursive Systematic Convolutional Transducers Based on Single Shift Registers," IEEE Access, vol. 2, 2014 Digital Object Identifier 10.1109/ACCESS.2014.2316413.

[9] ETSI, 3GPP TS 36.212: "Evolved Universal Terrestrial Radio Access (E-UTRA), Multiplexing and channel coding". http://www.etsi.org/deliver/etsi_ts/136200_136299/136212/08.08.00_60/ts_136212v080800p.pdf

[10] European Telecommunications Standards Institute, Digital Video Broadcasting (DVB); Second Generation, DVB Interactive Satellite System; Part2: Lower Layers for Satellite Standard,DVBdocument A155-2, Mar. 2011.

[11] C. Weiss, C. Bettstetter, S. Riedel, and D.J. Costello, "Turbo decoding with tailbiting trellises". Proc. IEEE Int. Symp. Signals, Syst., Electron., Pisa, Italy, pp. 343-348, Oct. 1998.



SEEK DIGITAL LIBRARY

[12] W. Koch and A. Baier, "Optimum and sub-optimum detection of coded data disturbed by time-varying intersymbol interference, " in *Proc. IEEE GLOBECOM*, San Diego, CA, USA, Dec. 1990, pp. 1679_1684.

[13] H. Balta, C. Douillard, "On the Influence of the Extrinsic Information Scaling Coefficient on the Performance of Single and Double Binary Turbo Codes", Advances in Electrical and Computer Engineering Volume 13, Issue: 2, pp.: 77-84, 2013.

[14] A Matache, S Dolinar, F Pollara, Stopping rules for turbo decoders, TMO Progress Report 42–142, Jet Propulsion Laboratory, Pasadena, California, 2000.

About Author (s):

MARIA KOVACI was born in Timisoara, Romania, in 1972. She received the B.S., M.S.and Ph.D. degrees in electronics and telecommunications engineering from University Politehnica Timisoara, Romania, in 1998 and 2009, respectively.

Since 2013, she has been an Assistant Professor with the Communications Department, University Politehnica Timisoara. Her main research interests include interleavers design, turbo codes, flat fading wireless channels and signal processing.

HORIA BALTA was born in Timisoara, Romania, in 1966. He received the B.S. and M.S. degrees in electronics and telecommunications engineering from the "Gheorghe Asachi" Technical University of Iasi, Romania, in 1990, and the Ph.D. degree in electronics and telecommunications engineering from University Politehnica Timisoara in 2008.

Since 2008, he has been an Assistant Professor with the Communications Department, University Politehnica Timisoara. His research interests include information theory, error correcting codes, in particular, turbo codes, and signal processing.



SEEK DIGITAL LIBRARY